Pergamon

Tetrahedron 56 (2000) 143–156

TETRAHEDRON

Phosphiranes as Ligands for Platinum Catalysed Hydrosilylations

Jürgen Liedtke, Sandra Loss, Christoph Widauer and Hansjörg Grützmacher*

Laboratory of Inorganic Chemistry, ETH-Zentrum, Universitätsstrasse 6, CH-8092 Zürich, Switzerland

Received 28 April 1999; accepted 2 August 1999

Abstract—The stability of phosphiranes can be enhanced by inclusion of the PC_2 ring into a polycyclic framework. *BABAR*-Phos type phosphiranes are easily prepared in high yield, they are thermally stable and allow the synthesis of various platinum(0) complexes. In contrast to other platinum(0) phosphine complexes, these are active hydrosilylation catalyst precursors. The reversible insertion of an electron rich metal centre into one P–C bond of the phosphirane ring was demonstrated for the first time.

Introduction

The elemental steps, i.e. oxidative addition of E–H to an unsaturated transition metal fragment (a), co-ordination of an olefin (b), insertion (c), and reductive elimination (d), of a catalysed addition of an element hydride bond, E–H, to a C=C bond system are recalled in a simplified manner in Scheme 1.

It is often assumed that the last step (d), i.e. the formation of the E–C bond, has the highest activation barrier and determines the overall rate and efficiency of the process.[1] Reductive elimination is favoured when the metal centre has a formally high oxidation state. For a given metal centre and substrates E–H and C=C, the only way to influence the electron density on the metal lies in the choice of the appropriate phosphine ligand. Under such conditions, an electron withdrawing phosphine PR_3 may accelerate the catalytic reaction (note however that the first step, the oxidative addition (a), requires an electron rich metal centre and this rate may become slower). Apart from using electronegative substituents on the phosphorus centre one might think about altering the bond angles.

This approach is illustrated in Scheme 2, showing simple MO diagrams for eight valence electron AH_3 species, which result when a planar form (D_{3h}) is converted into a pyramidal form (C_{3v}).

It is clear that a planar phosphine (D_{3h} symmetry) shall have good σ-donating but poor π-accepting properties since its HOMO and LUMO lie quite high in energy. Remember that the electron accepting orbitals on the metal lie higher in energy than the ligand donating orbitals and the electron donating metal centred orbitals lie lower in energy than the ligand centred acceptor orbitals.

When the phosphorus becomes pyramidalised, the HOMO, which is a pure p_z orbital in D_{3h}, decreases in energy. At the same time the energy of the degenerate set of anti-bonding orbitals strongly decreases with increasing pyramidalisation which eventually become the LUMOs of an AH_3 molecule in C_{3v} symmetry. These orbitals are responsible for the π-accepting properties of the phosphine.[2] Phosphiranes are the most strongly pyramidalised phosphines known (Σ°(P): 240–275)[3] which, according to Scheme 2, should make them excellent π-acceptors and promising ligands in transition metal catalysed reactions where step (d) is rate determining.

Phosphiranes may be synthesised using different methods which are briefly summarised in Scheme 3.[3] The condensation reaction (a) is the most obvious approach[4a–f] and has recently been used to prepare chiral phosphiranes stereoselectively.[4b] Another elegant way of synthesising chiral phosphiranes has been found by reacting oxiranes with PR^1 transfer reagents.[4d–f]

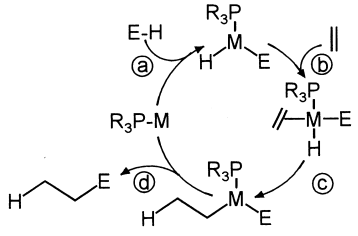

Scheme 1. Simplified catalytic cycle showing the addition of an E–H bond to a C=C bond.

Keywords: catalysis; hydrosilylation; phosphorus; phosphiranes; platinum.
* Corresponding author. Tel.: +41-1-632-2855; fax: +41-1-632-1090; e-mail: gruetz@elwood.ethz.ch

0040–4020/00/$ - see front matter
PII: S0040-4020(99)00783-8

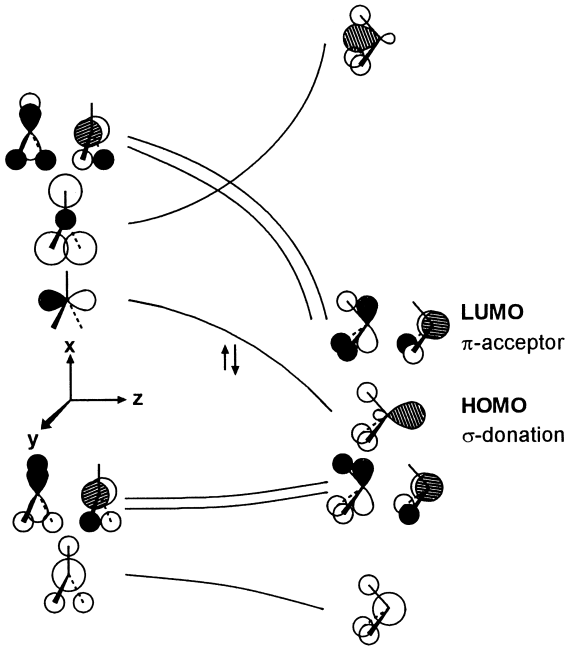

Scheme 2. Walsh diagram for the conversion of a trigonal planar AH_3 molecule (D_{3h}) into a pyramidal AH_3 molecule (C_{3v}).

Functionalized phosphiranes were prepared using method (b) in which a highly reactive phosphandiyl metal complex generated in situ is added in a [2+1] cycloaddition reaction to an olefin or to an allene.[4g,h] Related to this synthesis is the addition of a carbene to a phosphaalkene [eq. (c)].[4i–p] In these reactions, intermediates **A** (when a diazo compound is used as carbene source) and/or **B** which undergoes a conrotatory electrocyclic ring closure frequently have been observed or even isolated. Using method (c), alkylidene phosphiranes[4k–m] and bicyclic phosphiranes[4o] were obtained. A cycloaddition–cycloreversion sequence was used to prepare thio-phosphiranes with a PSC ring skeleton.[4q] Recently, reaction (d) has been described which allows the synthesis of C-functionalized phosphiranes.[4r]

Phosphiranes are quite reactive entities and are in particular photolytically labile and may undergo either [2+1] cycloreversion reactions,[3a–c,5a,b] retro-electrocyclisation,[5c] or ring–chain rearrangement reactions.[4f,5d–h] The ring opening polymerisation of the phosphirane $(Mes^*P)(CH_2)_2$ (Mes^*=2,4,6-*t*BuC_6H_2) gave polymers with molecular weights up to 7800.[5h] The lability of phosphiranes may be one reason why their use in transition metal catalysed reactions was found to be limited although initial promising results were obtained in asymmetric hydrogenations.[6] Phosphiranes, in which the PC_2-ring is embedded in a polycyclic framework are considerably more stable[7a–e] and a

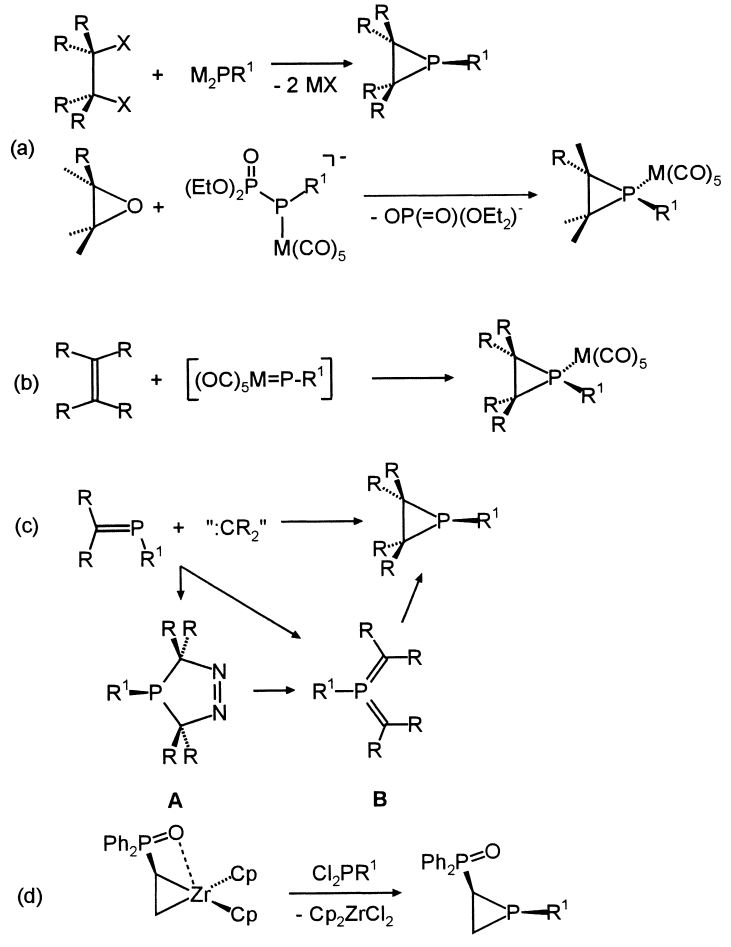

Scheme 3. Representative examples for the synthesis of phosphiranes.

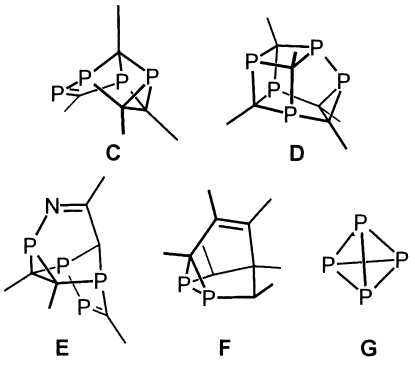

Scheme 4. Representative examples of polycyclic cage compounds containing PC_2, P_2C, and P_3 rings.

representative collection of such phosphiranes is shown in Scheme 4.

Results and Discussion

Synthesis of phosphiranes (*BABAR*-Phos) and a phosphiranium salt

We searched for a simple high yield synthesis of phosphiranes, in which the PC_2-ring is embedded in a polycyclic framework. In a preliminary communication we described such phosphiranes, which we named *BABAR*-Phos.[8] They are easily prepared in excellent yields starting from the dibenzoannulated tropolone **1**, which is converted via the chloride **2** to the amines **3a–c**. After lithiation and subsequent reaction with PCl_3 the dichloroaminophosphanes **4a–c** are isolated as colourless crystals in >90% yield. Using commercially available magnesium turnings and THF as solvent, dehalogenation of **4a**,**b** leads to gram quantities of the aminosubstituted phosphiranes **5a**,**b** (>90%) (Scheme 5). They form colourless crystals, which melt without decomposition and can be handled in air. Neither the pentafluorophenylsubstituted dichlorophosphane **4c** nor the phosphirane **5c** are very stable compounds. Compound **4c** undergoes a noteworthy rearrangement reaction to give the iminophosphorane **6**. This reaction proceeds slowly in the solid state at room temperature (several days) but is complete in solution after several minutes at about 60°C. Phosphirane **5c** could not be isolated but was characterised in solution by NMR spectroscopy. It polymerises upon concentration of the reaction solution to yield an as yet undefined colourless gum like material. We ascribe both reactions to the enhanced polarity of the N–C bond in **4c** or P–C bonds in **5c**, respectively (see Table 3 below).

Formally the phosphiranes **5a–c** are formed by an intramolecular [2+1] cycloaddition of an R_2N–P phosphinidene unit to the C=C double bond of the central seven-membered ring of the dibenzotropylidene unit which has a rigid boat conformation. Because of the low reactivity of triplet phosphinidenes, this approach has found little application in intermolecular cycloaddition reactions for the preparation of phosphiranes.[3,5b,i] In contrast to 1-phenylphosphirane, **5a**,**b** do not react with strongly alkylating agents such as $MeOSO_2CF_3$ to form phosphiranium salts.[9] However,

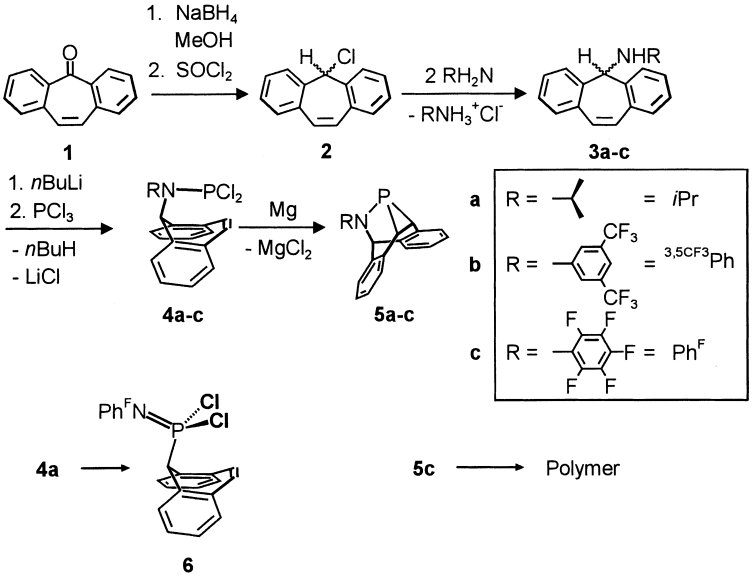

Scheme 5. Synthesis of phosphiranes **5a**–**c**.

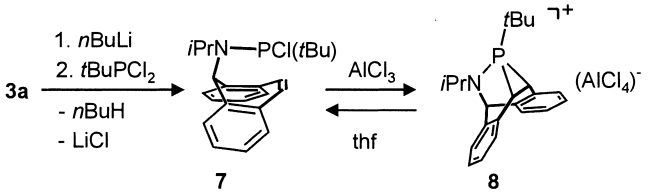

Scheme 6. Synthesis of phosphiranium salt **8**.

Table 1. Selected B3LYP/6-31G(d) bond lengths [Å] and angles [°] for the phosphiranes **I–V**

	N–P	P–C^4	P–C^5	C^4–C^5	NPC^4	NPC^5	C^4PC^5	P$C^4$$C^5$	P$C^5$$C^4$
I	1.745	1.851	1.873	1.513	101.3	105.2	47.9	66.8	65.3
II	1.641	1.808	1.808	1.531	119.1	119.1	50.1	65.0	65.0
III	1.733	1.917	1.870	1.546	99.8	98.1	48.2	64.3	67.5
IV	1.663	1.823	1.796	1.610	110.1	107.2	52.8	62.7	64.4
V	1.748	2.826	1.889	1.522	88.5	99.5	30.1	38.5	111.5

Table 2. Selected atomic charges derived from the natural population analysis of the compounds **III–V**[a]

	C^1	C^2	C^3	C^4	C^5	C^6	C^7	N	P
III	−0.131	−0.253	−0.230	−0.528	−0.540	−0.227	−0.214	−0.971	0.947
IV	−0.135	−0.207	−0.239	−0.511	−0.528	−0.231	−0.187	−0.962	1.415
V	−0.112	−0.483	−0.244	−0.459	−0.577	−0.263	−0.262	−0.989	0.707

[a] The NBO analyses were calculated at the B3LYP/6-31G(d) level.

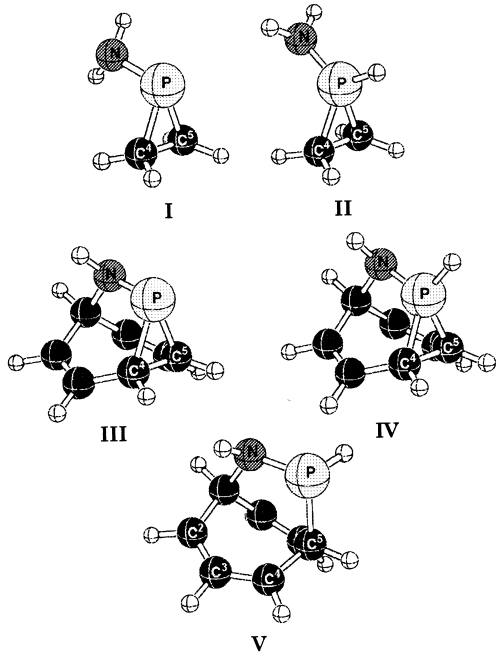

Figure 1. Schematic representation of the compounds **I–V** optimised at the B3LYP/6-31G(d) level.[†]

chloride abstraction from **7**, which was synthesised from lithiated **3a** and *t*$BuPCl_2$, by $AlCl_3$ in methylene chloride as solvent, cleanly afforded the phosphiranium salt **8** as colourless crystals (Scheme 6).

In analogy to the preparation of phosphiranes **5a–c**, this reaction corresponds to an original intramolecular [2+1] cycloaddition of a phosphenium ion, R_2P^+, to a C=C double bond. The reverse reaction, i.e. transfer of R_2P^+ units from phosphiranium salts is documented.[9a,b] Addition of THF to a solution of **8** reverses the halide abstraction and starting material **7** is reformed.

Computational results

In order to gain insight into the electronic structure of

[†] Selected geometrical parameters are given in Table 1.

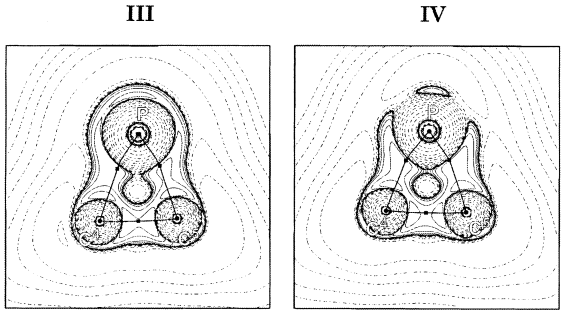

Figure 2. Two dimensional plots of the Laplace distribution for compounds **III** and **IV**, in a plane containing the atoms of the three-membered ring P, C^4 and C^5, respectively.[‡]

BABAR-Phos **5a–c** and the phosphiranium salt **8**, we performed DFT calculations on the B3LYP/6-31G(d) level for the model compounds **I–V**. A depiction of the structures of **I–V** is given in Fig. 1 and pertinent bond lengths and angles are listed in Table 1.

The results of the topological analysis of the charge density of the parent amino substituted phosphirane **I** are in good agreement with the results previously reported for the phosphirane $HP(CH_2)_2$.[10] As was found there, the P–C bonds are highly polar as can be seen from the location of the bond critical points r_b (Table 3) which are non-symmetrically placed on the P–C bond paths being closer to the phosphorus centre. Protonation of the phosphorus lone pair leads to **II** whereby only small variations of the P–C bond properties are observed. The C–P bonds become slightly shorter whereas the C–C bond length increases from 1.515 to 1.533 Å (Table 1). In Table 2, atomic charges of **III–V** derived from a NBO analysis are listed. In Fig. 2, the Laplace fields in the PC_2 plane of *BABAR*-Phos model **III** are compared with the phosphiranium salt **IV** and the results of a topological analysis of the charge densities of all compounds **I–V** are given in Table 3.

[‡] The electron densities were calculated at the B3LYP/6-31G(d) level. In the graphical representation $-\nabla^2\rho$ is drawn, so that local concentration is expressed by a positive value (solid lines) and local depletion is expressed by a negative value (dashed lines). Bond critical points are indicated by black squares.

Table 3. Selected results of the topological analysis of the charge density of the compounds **I**–**IV**[a]

	Bond	A–B [Å]	r_b	A-r_b [Å]	ρ_b [e Å^{-3}]	$\nabla^2\rho_b$ [e Å^{-5}]	H(r_b) [h Å^{-3}]	ϵ_b
I	P–N	1.745	0.383	0.669	1.02	7.54	−0.78	0.10
	P–C^4	1.870	0.391	0.731	0.98	−3.05	−0.91	0.49
	P–C^5	1.891	0.395	0.746	0.94	−3.16	−0.85	0.62
	C^4–C^5	1.515	0.498	0.755	1.65	−12.00	−1.34	0.23
II	P–N	1.641	0.387	0.636	1.22	15.04	−0.93	0.09
	P–C^4	1.828	0.397	0.726	1.09	−5.44	−1.08	0.65
	P–C^5	1.828	0.397	0.727	1.09	−5.44	−1.08	0.65
	C^4–C^5	1.533	0.500	0.766	1.62	−11.60	−1.30	0.18
III	P–N	1.733	0.383	0.664	1.05	8.40	−0.82	0.13
	P–C^4	1.930	0.424	0.818	0.88	−4.11	−0.71	0.58
	P–C^5	1.887	0.403	0.761	0.96	−4.49	−0.87	0.39
	C^4–C^5	1.547	0.498	0.771	1.54	−10.33	−1.18	0.24
IV	P–N	1.663	0.385	0.640	1.22	12.44	−0.99	0.24
	P–C^4	1.844	0.408	0.751	1.07	−6.44	−1.04	0.48
	P–C^5	1.814	0.391	0.709	1.13	−4.57	−1.14	0.42
	C^4–C^5	1.611	0.500	0.805	1.38	−7.88	−0.98	0.25

[a] r_b is the location of the bond critical point given in the ratio of distances A-r_b/A–B; A-r_b is the distance of the bond critical point r_b to the atom A; ρ_b and $\nabla^2\rho_b$ give the electron density and the second derivative at the bond critical point; H(r_b) gives the energy density at the bond critical point; ϵ_b the ellipticity at the bond critical point.

However, the Laplacian $\nabla^2\rho_b$ of the P–N bond strongly increases from 7.5 to 15.0 e Å^{-5}. This reflects the increasing dipolar nature of the covalent $P^{\delta+}$–$N^{\delta-}$ bond due to the more electropositive P atom in **II**.

The corresponding results for **III** and **IV** are analogous with one remarkable exception. Protonation of *BABAR*-Phos **III** results in a significant increase of the C^4–C^5 bond length by 0.054 Å from 1.546 to 1.610 Å. This finding is in good agreement with the experimental value of 1.601(6) in **8** (vide infra). Accordingly, the charge density ρ_b at the ring critical point of the C^4–C^5 bond decreases in the order **III**>**IV**. This can be rationalised by the contraction of the P–N and C–P bonds in **IV**, which results in a higher ring strain in the phosphirane moiety.

As expected, protonation results in an increase of positive charge at the P-atom that rises from 0.95 in **III** to 1.42 in **IV**. The negative charges on the carbon atoms C^4 and C^5 are only slightly diminished. However, if the charges on the hydrogen atoms H^4 and H^5 are taken into account, a decrease of the negative group charges C^4–H^4 (−0.261 in **III** versus −0.197 in **IV**) and C^5–H^5 (−0.27 in **III** versus −0.21 in **IV**) is observed. This means that σ-charge transfer from P to H^4 and H^5 occurs in **IV**.

It is well known that phosphiranes underlie P–C bond rupture upon nucleophilic attack which takes place on the phosphorus centre.[3] We have therefore investigated the effect caused by the smallest 'nucleophile' accessible to chemists: a hydride. Indeed, in the corresponding anion **V** the C^4–P bond is broken when the geometry is optimised taking the structure of **III** as a starting point. In the B3LYP/6-31G(d) minimum structure the moiety C^2–C^3–C^4 (C^2–C^3 1.400 Å, C^3–C^4 1.403 Å) shows the typical bond characteristics of an allyl anion. Inspection of the atomic charges listed in Table 2 show that a considerable part of the extra negative charge is distributed over C^2–C^3–C^4. The rest of the additional negative charge is allocated on the N and C^5 centres while the charge at the P-atom remains positive. We conclude from our theoretical inspection of *BABAR*-Phos type ligands that these contain rather positively charged phosphorus centres that should make them electron-withdrawing ligands. Furthermore, positive as well as negative charge may be partially delocalised into the ligand framework.

Synthesis of catalyst precursors

In our previous investigation, we studied the binding qualities of *BABAR*-Phos ligands qualitatively by comparing the isolated and fully characterised d^{10} complexes [Cu(*^{iPr}BABAR*-Phos)$_2$(MeCN)$_2$]$^+$ and [Pt(*^{iPr}BABAR*-Phos)$_2$(PPh$_3$)$_2$] (*^{iPr}BABAR*-Phos=**5a**).[8] While the phosphirane **5a** [Σ°(P)<250] remains tightly bonded to the platinum centre it is readily displaced by Ph$_3$P [Σ°(P)≈303] from the copper complex. This observation is in accord with the assumption that *BABAR*-Phos ligands are worse σ-donors but better π-acceptors than Ph$_3$P. Given that platinum(0) olefin complexes are active hydrosilylation catalysts,[1d] the mono *BABAR*-Phos complexes **11a**,**b** were prepared.[8] While **11a** could be obtained in pure form as slightly yellow crystals, the isolation of larger amounts of pure **11b** failed. However, **11b** was characterised by multi-nuclear NMR spectroscopy in solution in presence of excess divinyltetramethylsiloxane (dvtms). Furthermore, single crystals suitable for an X-ray analysis were obtained (vide infra). In order to investigate the effect of the co-ordinated olefin on the catalyst performance, we also prepared the new maleic anhydride **12** (malan) complex **13** as shown in Scheme 7.

This new complex forms two isomers, **13** and **13′**, in solution. It crystallises in the form of isomer **13**, which, in solution, slowly gives back a 5/1 equilibrium mixture of **13** and **13′**. We assume that **13′** differs from **13** by a 180° rotation of the maleic anhydride ligand, however, a concomitant rotation of the *BABAR*-Phos ligand can not be excluded. In contrast to **11a**,**b** where both halves of the ligand show identical ^{1}H and ^{13}C NMR signals, all ^{1}H and ^{13}C nuclei are different in **13**, **13′** giving rise to very complex spectra but indicating that any exchange phenomena

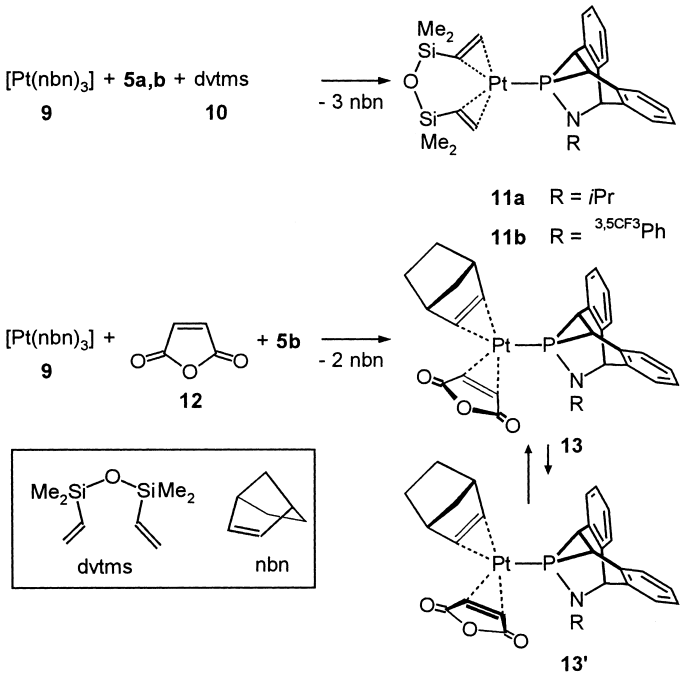

Scheme 7. Preparation of *BABAR*-Phos Platinum(0) olefin complexes.

is slow on the NMR time scale. Crystalline **13** is colourless and stable in air.

In the ^{31}P NMR spectra of **11a**,**b** and **13**,**13′**, one resonance signal at about −80 ppm is observed which is approximately Δ70 ppm shifted to higher frequencies when compared to the unbounded *BABAR*-Phos ligands **5a**–**c** (≈−150 ppm). The $^{1}J(^{195}Pt^{31}P)$ coupling constants (≈4200 Hz) lie in the upper range of values observed for platinum(0) complexes.[11] However, they compare well with couplings which have been observed for the bis(phosphirene) complex {$Pt(PPh_3)_2$[$PhP(CPh)_2$]} ($^{1}J^{195}Pt^{31}P$=4222 Hz) which could be characterised in solution below −40°C.[12] It seems that platinum(0) complexes containing an intact phosphirane or phosphirene ligand could never be isolated before.

Rearrangement reaction of 11b

When solutions of **11b** in a non-polar solvent like *n*-hexane or benzene are kept at room temperature, a lemon yellow powder starts to precipitate after about one hour. The new compound **21** is sufficiently soluble in THF to obtain NMR spectra . At room temperature very broad ^{31}P NMR signals are observed which sharpen at lower temperatures and split into two AMX spin systems. However, the ^{1}H NMR and ^{13}C NMR spectra remain very complex. Layering a concentrated THF solution of **21** with *n*-hexane led to crystals suitable for an X-ray analysis, which allowed unequivocally the determination of the structure as a binuclear mixed valent platinum(0) platinum(II) phosphido bridged complex [Pt_2(^{3,5CF3}*BABAR*-Phos)$_2$(η_2−^{3,5CF3}*BABAR*-Phos)(dvtms)] as shown in Scheme 8.

The intermolecular insertion of carbene isolobal electron rich metal centres, i.e. [Pt(0)$(PR_3)_2$] or [Pd(0)$(PR_3)_2$] fragments, into one P–C bond of phosphiranes or phosphirenes is a well documented reaction.[12,13] In analogy, one might propose the reaction of [Pt(^{3,5CF3}*BABAR*-Phos)$_2$] fragments with **11b** as a reaction path leading to **21**. However, more

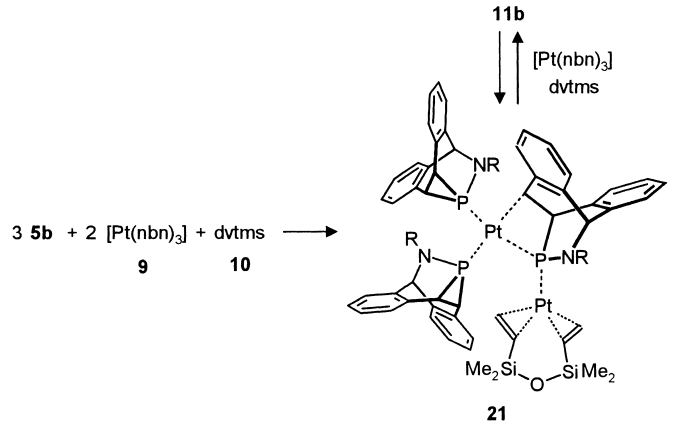

Scheme 8. Synthesis of **21**.

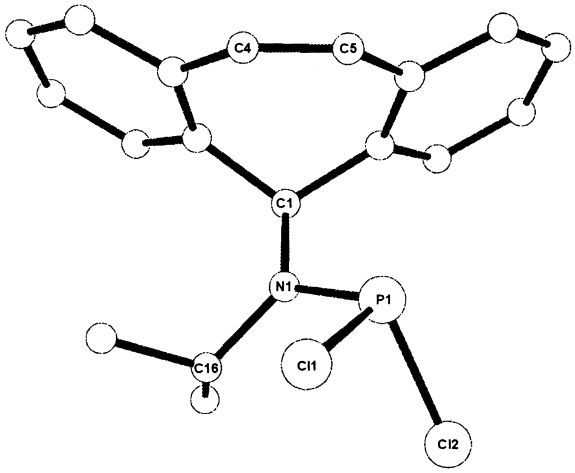

Figure 3. Molecular structure of dichlorophosphine **4a**. Selected bond lengths [Å] and angles [°]; P1–Cl1 2.078(1), P1–Cl2 2.117(1), P1–N1 1.640(2), N1–C1 1.503(3), N1–C16 1.500(3), C4–C5 1.337(4), Cl1–P1–Cl2 95.11(4), Cl1–P1–N1 101.52(9), Cl2–P1–N1 103.83(9), C1–N1–P1 118.4(2).

complex reaction steps involving ligand scrambling (which obviously occurs) and *intra*molecular insertion of Pt centres in P–C bonds cannot be ruled out at this stage of our investigations. Compound **21** can be prepared easily in high yield when the components **5b**, dvtms (**10**) and $[Pt(nbn)_3]$ (**9**) are mixed in benzene in the correct stoichiometry. Remarkably, when dvtms and **9** are added to a solution of **21**, complete

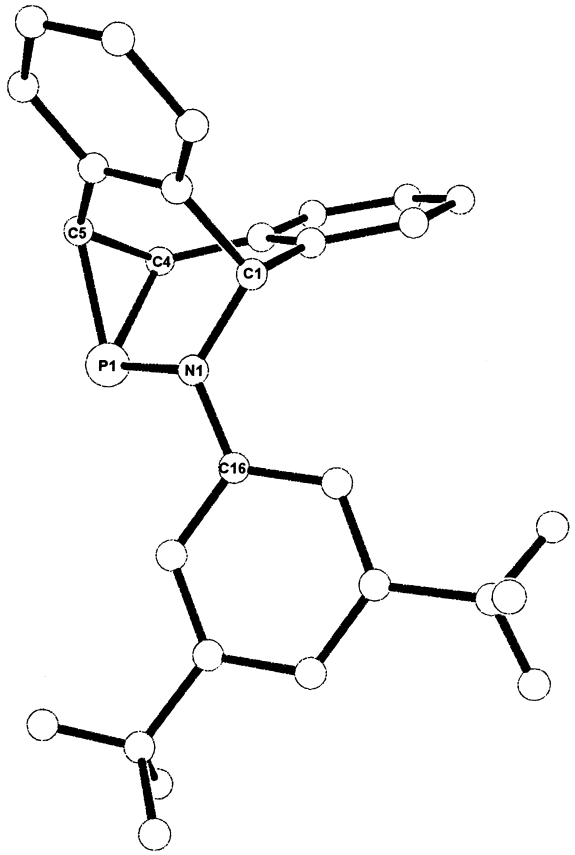

Figure 4. Molecular structure of *BABAR*-Phos **5b**. Selected bond lengths [Å] and angles [°] are listed in Tables 4 and 5, respectively.

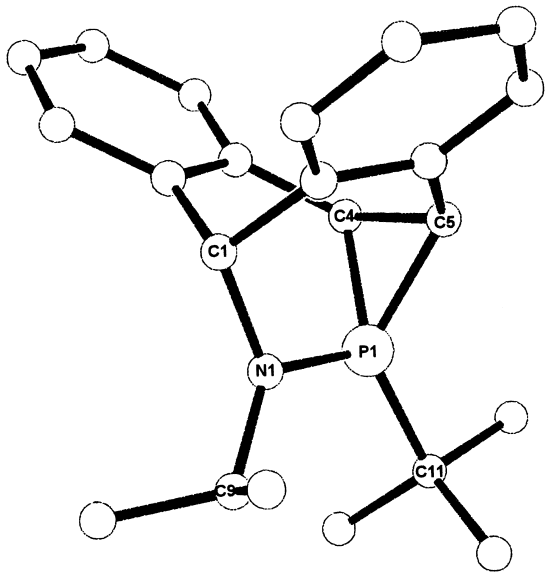

Figure 5. Molecular structure of the cation of phosphiranium salt **8**. Selected bond lengths [Å] and angles [°] are listed in Tables 4 and 5, respectively.

but slow reconstitution of **11b** is observed. This observation demonstrates for the first time that the metal insertion reaction into the P–C bond of a phosphirane can be reversible. We believe that this may be due to the particular electronic and steric properties of *BABAR*-Phos leading to a sufficiently small thermodynamic difference between the ring opened compound and intact PC_2 cycle *and* rather small activation barriers for the insertion and extrusion processes.

Preliminary two-dimensional NMR experiments lead us to assume that the complex NMR spectra of **21** are due to the formation of two different isomers in solution which interchange on the NMR time scale. Since the phosphorus nuclei of the intact *BABAR*-Phos ligand ($\delta \approx -75$) shows no cross-peak with the ^{31}P nucleus ($\delta \approx -45$) of the ring opened ligand, an equilibrium between these two can be excluded and the exchange process very likely consists of a hindered rotation around the Pt–P bonds of the *BABAR*-Phos ligands.

Molecular structures of 4a, 5b, 8, 11b, 13 and 21

We have characterised the dichlorophosphine **4a** (Fig. 3), *BABAR*-Phos **5b**[8] (Fig. 4), the phosphiranium salt **8** (Fig. 5), and the platinum complexes **11a**[8] and **11b** (Fig. 6), **13** (Fig. 7), and **21** (Fig. 8) by X-ray analyses.[14]

For comparison, selected bond lengths and angles of the *BABAR*-Phos framework in these compounds are listed in Tables 4 and 5, respectively. Further selected data are given in the figure captions. The bond parameters show some common expected trends: in all compounds the ring internal P–C bonds (a_1,a_2) and P–N (c) bonds become shorter when the P-lone pair is involved in bonding. At the same time, the basal C–C bond, b, becomes longer and the sum of bond angles, $\Sigma(P)^\circ = \alpha + \beta_1 + \beta_2$, at phosphorus becomes larger. These effects are most pronounced in the phosphiranium salt **8** where the lone pair at phosphorus becomes a covalent

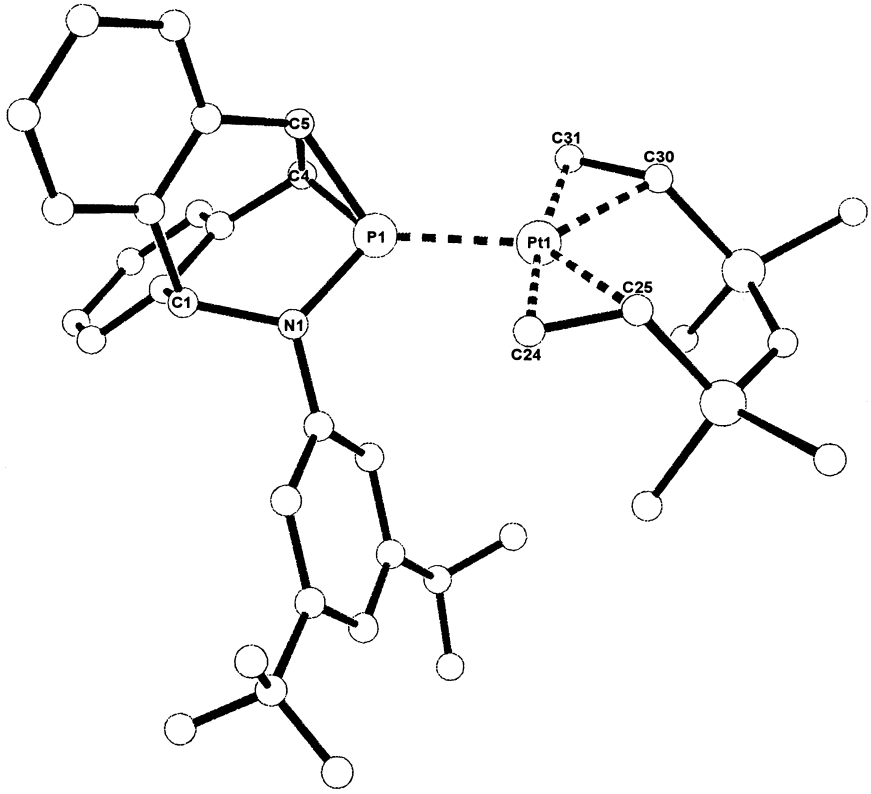

Figure 6. Molecular structure of **11b**. Further selected bond lengths [Å] and angles [°] are listed in Tables 4 and 5, respectively; X1 lies in the centre of the bond C24=C25, X2 in the centre of C30=C31, Pt1–C24 2.140(4), Pt1–C25 2.152(4), Pt1–C30 2.156(4), Pt1–C31 2.135(4), C24–C25 1.430(5), C30–C31 1.405(6), P1–Pt1–X1 113.2(2), P1–Pt1–X2 113.9(2), X1–Pt1–X2 132.7(2).

P–C σ-bond. The structural parameters of the *BABAR*-Phos unit of all platinum complexes regardless of formal oxidation state or co-ordination number are quite similar, i.e. Σ(P)° lies in a narrow range of 251–257; about 10° larger than in the unbound ligand **5b**. The Pt–P bond lengths in the three-co-ordinate platinum(0) complexes **11a**,**b** and **13** are somewhat shorter than the distances of the four-co-ordinate platinum(II) centre to the phosphorus centres of the

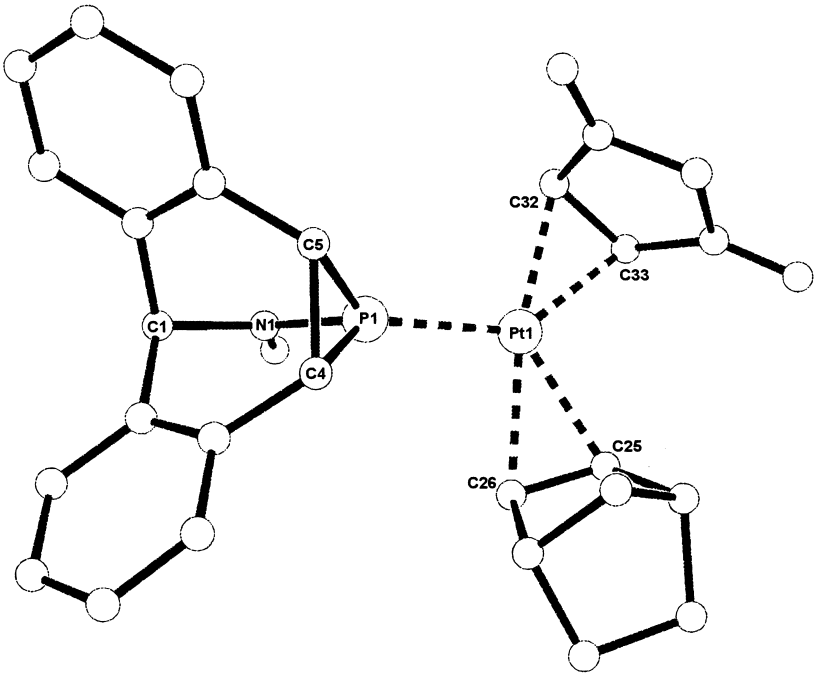

Figure 7. Molecular structure of **13**. Further selected bond lengths [Å] and angles [°] are listed in Tables 4 and 5, respectively. X1 lies in the centre of the bond C25=C26; X2 in the centre of C32=C33. The 3,5-$(CF_3)_2C_6H_3$ substituent on N1 has been omitted for clarity. Pt1–C25 2.17(1), Pt1–C26 2.19(1), Pt1–C32 2.10(1), Pt1–C33 2.08(1), C25–C26 1.38(2), C32–C33 1.42(2), P1–Pt1–X1 108.0(4), P1–Pt1–X2 121.9(4) X1–Pt–X2 130.1(4).

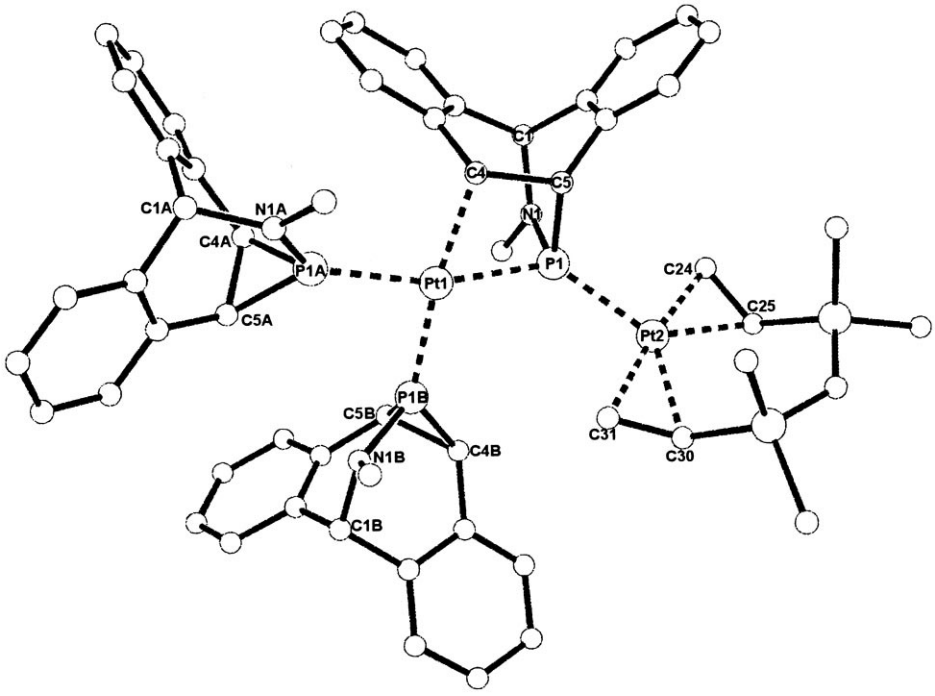

Figure 8. Molecular structure of **21**. Further selected bond lengths [Å] and angles [°] are listed in Tables 4 and 5, respectively; X1 lies in the centre of the bond C24=C25, X2 in the centre of C30=C31, P1–Pt1 2.333(2), P1–Pt2 2.274(2), P1–C4 2.542(2), P1–C5 1.832(8), Pt1–C4 2.120(8), C4–C5 1.550(11), N1–P1 1.738(7), Pt2–C24 2.133(10), Pt2–C25 2.152(9), Pt2–C30 2.150(9), Pt2–C31 2.122(9), C30–C31 1.410(12), C24–C25 1.418(13), P1A–Pt1–P1B 91.26(8), C4–Pt1–P1A 98.0(2), P1–Pt1–P1B 101.17(8), P1–Pt1–C4 69.3(2), Pt1–P1–N1 102.1(2), Pt1–P1–C5 86.0(3), N1–P1–C5 97.1(4), Pt1–P1–Pt2 130.6(1), P1–Pt2–X1 114.1(4), P1–Pt2–X2 111.6(4) X1–Pt2–X2 134.1(4). Sum of bond angles at P1: 285.2°.

Table 4. Selected bond lengths of the *BABAR*-Phos entities in **5b**, **8**, **11a,b**, **13** and **21**

	Z	a_1 [Å]	a_2 [Å]	*b* [Å]	*c* [Å]	*d* [Å]
5b[a]	–	1.850(3)	1.863(3)	1.532(4)	1.738(2)	–
8	*t*Bu	1.774(3)	1.774(3)	1.601(6)	1.628(4)	1.823(5)
11a[a]	Pt	1.812(6)	1.821(7)	1.576(9)	1.684(6)	2.241(2)
11b	Pt	1.811(4)	1.844(4)	1.544(6)	1.711(3)	2.231(1)
13	Pt	1.825(10)	1.827(10)	1.597(14)	1.682(10)	2.251(2)
21[b]	Pt1	1.811(8)	1.825(8)	1.561(12)	1.687(7)	2.295(2)

[a] See Ref. 8.
[b] Averaged data of both *BABAR*-Phos ligands are given; the largest difference being 0.04 between the Pt–P1A (2.313(2) Å) and Pt–P1B (2.277(2) Å) distances.

BABAR-Phos ligands in **21** [Pt–P1A (2.313(2) Å), Pt–P1B (2.277(2) Å], which reflects the sterical crowding in this complex. The longest Pt–P distance [2.333(2) Å] is found in **21** between the bridging phosphido centre P1 and the platinum(II) centre Pt1 which falls in the range of the Pt(0)– PPh_3 distances [2.324(1) Å] observed in [Pt(^{iPr}*BARBAR*-Phos)$_2$(PPh_3)$_2$].[8]

The structure of the ring opened phosphirane moiety in **21** merits some attention. Apart from the P–C distances, which became very different [P1–C5 1.832(8) Å; P1–C4 2.542(2) Å versus 1.811(8) Å and 1.825(8) Å for a_1 and a_2, respectively] as a consequence of the insertion reaction, other structural parameters remain remarkably constant (i.e. the N–P–C5 angles vary by 3° and the C–C distances within the C–C skeleton do not change significantly).

This is probably a consequence of the rigid polycyclic structure of the *BABAR*-Phos ligand and may explain the reversibility of the insertion reaction. The fold angle along the P1–C4 axis within the Pt1–P1–C4–C5 cyclobutane moiety amounts to 25.8°. Since the [Pt(^{3,5CF3}*BARBAR*-Phos)2(η_2-^{3,5CF3}*BARBAR*-Phos)] unit may be described as a phosphine ligand co-ordinating to the Pt2 centre

Table 5. Selected bond angles in **5b**, **8**, **11a,b**, **13** and **21**

	α [°]	β_1 [°]	β_2 [°]	Σ [°]	γ_1 [°]	γ_2 [°]	γ_3 [°]
5b[a]	48.8(1)	98.8(1)	99.0(1)	246.5	–	–	–
8	53.6(2)	108.2(2)	108.2(2)	269.9	119.7(2)	124.9(2)	124.9(2)
11a[a]	51.4(3)	101.7(3)	103.1(3)	256.2	119.8(2)	130.0(2)	131.4(2)
11b	50.0(2)	100.5(2)	101.4(2)	251.9	122.5(1)	125.4(1)	133.7(1)
13	51.8(5)	102.1(5)	103.3(5)	257.2	121.8(3)	130.5(4)	126.8(4)
21[b]	50.9(4)	101.0(4)	102.7(4)	254.6	124.4(3)	128.1(3)	125.8(3)

[a] See Ref. 8.
[b] Averaged data of both *BABAR*-Phos ligands are given; the largest difference being 0.04 between the Pt–P1A (2.313(2) Å) and Pt–P1B (2.277(2) Å) distances.

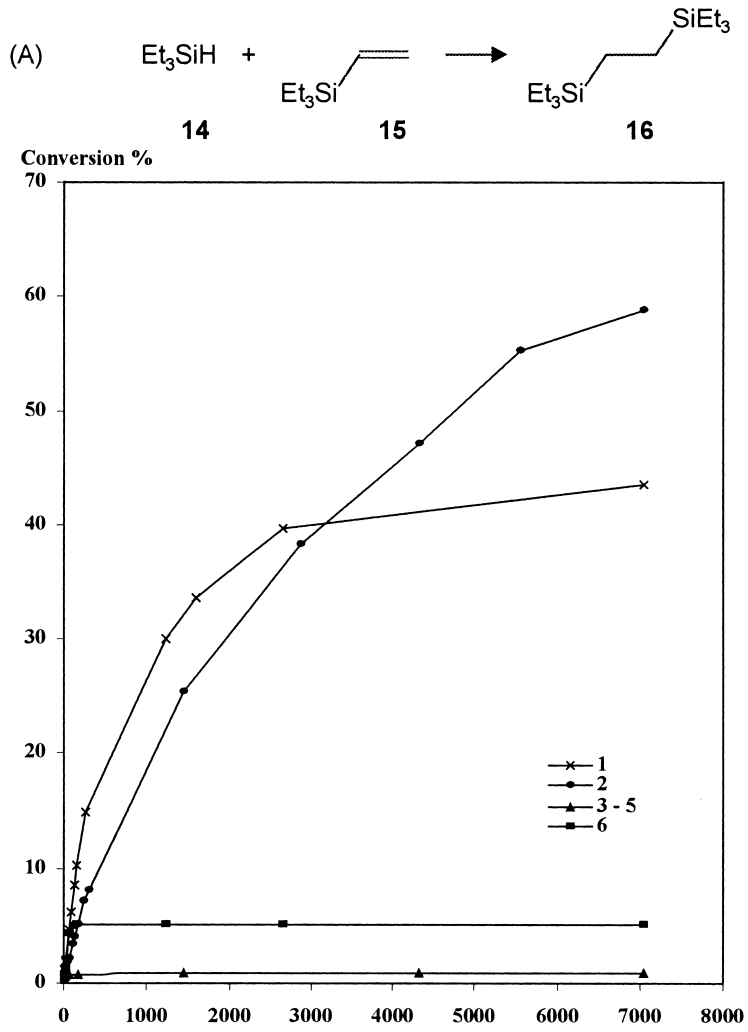

Figure 9. Hydrosilylation of triethylvinylsilane **15** with triethylsilane **14**. Conditions: 4 mmol **15**, 2 mmol **14**, 0.002 mmol catalyst ([Pt(nbn)$_3$] (**9**)/phosphine ratio=1:1.1). Catalyses: No. 1 (×): **9**/**5a**; No. 2 (●): **9**/**5b**; No. 3 (▲): **9**/P(OPh)$_3$; No. 4 (▲): **9**/P(N*i*Pr$_2$)Ph$_2$; No. 5 (▲): **13**; No. 6 (■): **9**/PPh$_3$.

we note the sum of bond angles around P1 which amounts to 285.2°.

Hydrosilylation reactions catalysed by platinum *BABAR*-Phos complexes

We have reported the use of *BABAR*-Phos **5a**,**b** as ligands for catalyst precursors in hydrosilylation reactions (A) (see Fig. 9) and (B) (see Fig. 10).[8] In these experiments, we mixed [Pt(nbn)$_3$] (**9**) with an excess of dvtms (**10**) prior to the addition of *BABAR*-Phos **5a**,**b** to afford catalyst precursors **11a**,**b**. By means of NMR spectroscopy, the complexes **11a**,**b** were the only platinum complexes detected in these solutions.

In order to exclude the possibility that the catalytic activity which we observed is not due to the high activity of [Pt$_2$(dvtms)$_3$] (Karstedt catalyst)[1d,15] which may be possibly present in small amounts, we have now altered slightly the protocol and performed the reactions without dvtms. Instead, we used a mixture of 1 equivalent [Pt(nbn)$_3$] (**9**) and 1.1 equivalents of a phosphine [i.e. **5a** in reaction no. 1, **5b** in reaction no. 2, P(OPh)$_3$ in reaction no. 3, P(N*i*Pr$_2$)Ph$_2$ in reaction no. 4 and PPh$_3$ in reaction no. 6] or isolated **13** (in reaction no. 5). In the solutions of **9** and **5a**,**b**, broad signals in the ^{31}P NMR spectra at about −70 ppm indicate exchange reactions in which probably differently substituted [Pt(*BABAR*-Phos)$_n$(nbn)$_m$] (*m*, *n*: 1–3) species are involved. These complexes were found to be unstable and could not be isolated. However, it can be clearly seen from Fig. 9, that platinum(0) phosphirane complexes show considerable catalytic activity in reactions (A) and (B). Specifically, no conversions were observed in reaction (A) with P(OPh)$_3$, or P(N*i*Pr$_2$)Ph$_2$ (reaction no. 3 and 4) or when the maleic anhydride complex **13** was used as catalyst precursor (reaction no. 5). When PPh$_3$ is employed as ligand, little conversion (≈5%) is seen initially but the reaction does not proceed any further.

The binuclear complex **21** also shows no catalytic activity in reaction (A). There are different possible reasons why neither platinum precursor complexes generated with phosphines bearing electron withdrawing substituents, i.e. P(OPh)$_3$ or P(N*i*Pr$_2$)Ph$_2$, or electron poor olefins nor the platinum complex **21** lead to catalytic active complexes.

One may be that the use of the phosphines PPh$_3$, P(OPh)$_3$, and P(N*i*Pr$_2$)Ph$_2$ leads to oligo(phosphine) complexes—eventually

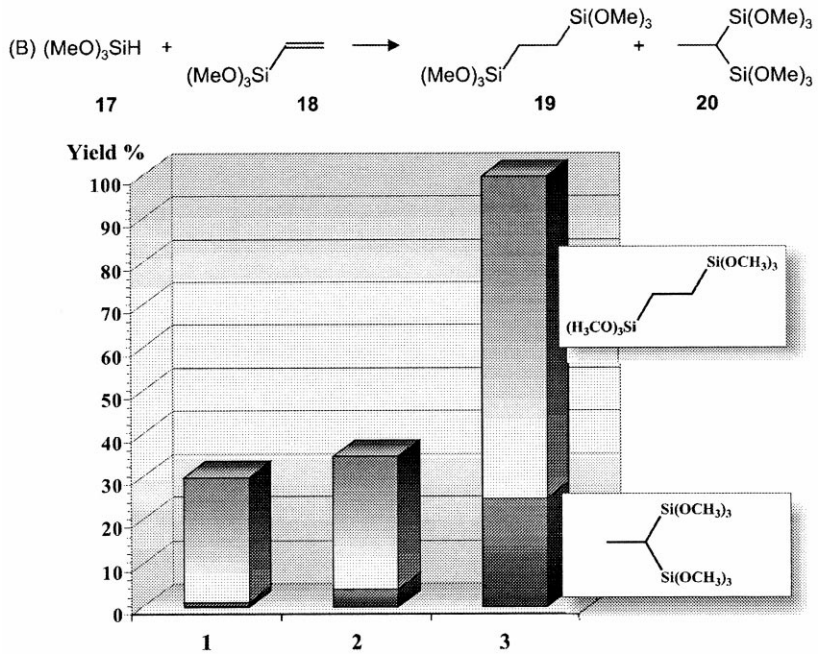

Figure 10. Hydrosilylation of trimethoxyvinylsilane **18** with trimethoxysilane **19**. Conditions: 1 mmol substrate, 0.5 mmol catalyst, C_6D_6 as solvent. Catalyses: no. 1: **9**/**5b**; No. 2: **9**/**5a**; No. 3: $[Pt_2(dvtms)_3]$.

in the course of the catalytic reaction—in which free co-ordination sites for the substrate molecules are blocked. Such $[Pt(PR_3)_nL_m]$ species are expected to be less substitution labile than simple platinum(0) olefin complexes. Also in line with this assumption is the observation that the maleic anhydride complex **13** is inactive. Probably due to the high affinity of the electron poor olefin **12** towards the platinum centre, the oxidative addition and/or co-ordination of the olefin becomes hampered [step (a) and (b) in Scheme 1, respectively].

Another reason, however, may indeed be that the particular electronic properties, i.e. the small sum of bond angles at the phosphorus centre in *BABAR*-Phos complexes, lead to more active phosphine complexes. The (reproducible) drop off of the reaction rate after approx. 2000 min using **9** and **5b** as the catalytic system may be explained by the inactivity of **21**, which may form in the course of the catalysis reaction. In this binuclear complex the ring opened phosphirane behaves like an 'ordinary' phosphine [Σ°(P1)=285] towards the Pt(0)(dvtms) moiety. In preliminary work we have already shown that the dvtms complex $[Pt(PPh_3)(dvtms)]$ is catalytically inactive.[8] Since the reconstitution of catalytically active *BABAR*-Phos species from **21** in the presence of other labile platinum(0) complexes—which may be present in solution—is quite slow, a decrease of the conversion rate is the consequence. Note that we have so far no evidence that a phosphirane ring opening reaction occurs when the N-isopropyl substituted *BABAR*-Phos ligand **5a** is employed and hence no unusual decrease in activity is observed.

In Fig. 10 the results for the catalysed hydrosilylation reaction of tri(methoxy)vinyl silane **18** with trimethoxysilane **17** are shown [reaction (B)]. As catalyst precursors 1:1.1 mixtures of **9**/**5b** (reaction no. 1); **9**/**5a** (reaction no. 2), and the Karstedt catalyst $[Pt_2(dvtms)_3]$ (reaction no. 3) were used. In the hydrosilylation reaction (B) two isomers, **19** and **20**, are obtained as products. As can be seen from the comparison, the Karstedt catalyst is still significantly more active but, as expected, less selective than the platinum(0) *BABAR*-Phos precursors. Note, however, that in contrast to reactions with Karstedt catalyst, we did not observe the formation of elemental platinum with *BABAR*-Phos platinum complexes. This observation indicates the higher stability of *BABAR*-Phos platinum complexes, which is an important issue in view of efforts directed towards the recycling of the catalyst. Qualitatively, all results obtained in this work resemble the ones we observed when all catalyses were carried out in the presence of dvtms whereby platinum(0) phosphine dvtms complexes are formed as precursors.[8]

Conclusion

We have shown that phosphiranes are interesting as ligands in transition metal catalysed reactions. Specifically, catalytic reactions in which reductive elimination is the overall rate determining step, may profit from the particular electronic properties of phosphiranes (i.e. a relatively high positive charge on the phosphorus centre and low lying π-acceptor orbitals). The approach of incorporating the PC_2 cycle within a rigid polycyclic framework may prove to be fruitful in order to suppress undesired side reactions. Thus we could demonstrate that the insertion of electron rich metal centres in one P–C bond is reversible. It will be particularly interesting to search for *BABAR*-Phos ligands in which the insertion and extrusion in one P–C bond is even more facile. This would allow development

Table 6. Selected NMR and physical data of **4a**–**c**, **5a**–**c**, **6**, **7**, **8**, **11a**,**b**, **13** and **21**[a]

	δ ^{31}P	δ ^{195}Pt	δ ^{1}H PC*H*C*H*	δ ^{13}C PC*H*C*H*	m.p. [°C]
4a	169		7.12	130.7	114
4b	155		7.21	130.6	122
4c	162		7.25	130.6	–
5a	−154		2.65, d, $^{2}J_{PH}$=22	21.3, d, $^{1}J_{PC}$=38	85
5b	−146		3.12, d, $^{2}J_{PH}$=20	22.4, d, $^{1}J_{PC}$=38	147
5c	−146, t, $^{4}J_{FP}$=41		3.23, d, $^{2}J_{PH}$=21		
6	5		7.05	131.5	–
7	160		7.11, 7.12, J_{AB}=12	130.5,d, $^{5'}J_{PC}$=1;131.6, d, $^{5}J_{PC}$=2	125
8	−16		4.38, d, $^{2}J_{PH}$=4.8	21.5, d, $^{1}J_{PC}$=8	133
11a	−74, $^{1}J_{PtP}$=4203	−3688, d, $^{1}J_{PPt}$=4203	2.85, $^{2}J_{PH}$=5.7, $^{3}J_{PtH}$=13.8	23.1, $^{1}J_{PC}$=15, $^{2}J_{PtC}$=18	(dec.)>95
11b	−77, $^{1}J_{PtP}$=4215	−3616, d, $^{1}J_{PPt}$=4215	3.02, m, $^{2}J_{PH}$=6.0, $^{3}J_{PtH}$=12	25.3, d, $^{1}J_{PC}$=18, $^{2}J_{PtC}$=14	(dec.) >85
13	−77, $^{1}J_{PtP}$=4247	−7169, d, $^{1}J_{PPt}$=4247	3.20, m, $^{3}J_{HH}$=4.5, $^{2}J_{PH}$=11.7, $^{3}J_{PtH}$=16; 3.7, m, $^{3}J_{HH}$=4.5, $^{2}J_{PH}$=11.7, $^{3}J_{PtH}$=12	21.4, d, $^{1}J_{PC}$=15, $^{2}J_{PtC}$=16; 23.3, d, $^{1}J_{PC}$=12, $^{2}J_{PtC}$=12	(dec.)>165
21[a]	−46, m, $^{1}J_{PtP}$=3201, $^{1}J_{PtP}$=1599, $^{2}J_{PP}$=211 (P1); −80, m, $^{1}J_{PtP}$=1960, $^{2}J_{PP}$=211, $^{2}J_{PP}$=16 (P1A); −88, m, $^{1}J_{PtP}$=2090, $^{3}J_{PtP}$=84 (P1B).	−5416, m			(dec.)>163

[a] Only the NMR data of the major isomer are given.

of catalysts in which the metal centre is parked within the ligand during the resting state but pulled out by substrate molecules during the active state.[16]

Experimental

The preparation of *BABAR*-Phos **5a**,**b** and complexes **11a**,**b** has been briefly reported before.[8] Selected NMR and physical data of the compounds described in this work are listed in Table 6.

Dibenzotropylidene amines 3a, 3b, 3c. The chloride **2** was prepared as described in the literature.[17] To a solution of 5.41 g **2** (23.8 mmol) in 500 ml toluene, 47.6 mmol of the corresponding primary amine RNH_2 (R=*i*Pr, 3,5-$(CF_3)_2C_6H_3$, F_5C_6) were added under a dry atmosphere. After about 1 h a white precipitate of amine hydrochloride has formed. Subsequently 200 ml of saturated aqueous Na_2CO_3 was added to the mixture. The organic phase was separated and the aqueous phase extracted three times with 200 ml of diethyl ether. The combined organic layers were dried over sodium sulphate and the solvents were removed under reduced pressure. The crude products were re-crystallised from hexane to give 85–95% of the pure colourless amines.

3a (a slow equilibrium at T=298 K between *endo* and *exo* isomer[17] of amine **3a** is established by the doubling of the ^{1}H and ^{13}C resonances): ^{1}H NMR ($CDCl_3$): δ 0.92, 1.13 (d, $^{3}J_{HH}$=6.20 Hz, C*H*$_3$, 6H), 1.93 (broad, s, N*H*, 1H), 2.24, 2.91 (sept, $^{3}J_{HH}$=6.20 Hz, C*H*$_{i\mathrm{Pr}}$, 1H), 4.27, 4.94 (s, C*H*, 1H), 7.04, 7.16 (s, C*H* olefin, 2H), 7.25–7.45 (m, C*H* aryl, 8H). ^{13}C NMR ($CDCl_3$): δ 22.45, 23.32 (s, C_b), 44.48, 45.84 (s, C_a), 57.31, 66.21 (s,C_1), 122.28, 125.44, 126.86, 127.59, 128.45, 128.66, 129.42, 129. 95, 130.45, 131.12 (s, C_4, C_8, C_9, C_{10}, C_{11}), 133.15, 133.88, 139.99, 140.66 (s,C_2, C_3).

3b (due to *endo exo* isomerisation all resonances are exchange broadened at T=298 K[17]): ^{1}H NMR ($CDCl_3$): δ 4.88 (broad, s, N*H*), 5.75 (broad, s, C*H*), 7.04 (s, C*H* olefin, 2H), 7.2–7.7 (m, C*H* aryl, 10 H). ^{13}C NMR ($CDCl_3$): δ 63.89 (broad s, C_1), 110.16 (broad s, C_a), 112.59 (broad s, C_b), 123.39 (q, $^{1}J_{FC}$=272.7 Hz, C_e), 127.35 (broad, s, C_d), 128.74, 129.98, 130.58, 132,99, 137.22 (s, C_4, C_8, C_9, C_{10}, C_{11}), 131.74 (q, $^{2}J_{FC}$=32.6 Hz, C_c), 147.31 (s, C_2 or C_3). ^{19}F NMR ($CDCl_3$): δ −63.5 (s).

3c (due to *endo exo* isomerisation all resonances are exchange broadened at T=298 K[17]): ^{1}H NMR ($CDCl_3$) δ 4.82 (broad, s, N*H*), 5.91 (broad, s, C*H*), 7.32 (s, C*H* olefin, 2H), 7.34–7.77 (m, C*H* aryl, 8 H). ^{13}C NMR ($CDCl_3$): δ 65.79 (broad s, C_1), 121.80 (broad s, *C*F), 122.04 (broad s, *C*F), 127.46 (s, C_a), 128.23, 128.35, 128.68, 129.00, 130.36 (s, C_4, C_8, C_9, C_{10}, C_{11}), 132.63 (s, C_2 or C_3), 135.65 (m, *C*F), 137.72 (s, C_2 or C_3).

General procedure for the preparation of the amino-dichloro phosphines 4a, 4b, 4c and 7. To a solution of the amine **3a**, **3b** or **3c** (40 mmol) in diethyl ether, 25 ml of a 1.6 M hexane solution of *n*BuLi (40 mmol) was added at −30°C. The reaction mixture was warmed to room temperature and then added dropwise to a solution of either PCl_3 (5 ml, 57 mmol) or *t*BuPCl_2 (3.8 g, 24 mmol) in 20 ml Et_2O at −20°C, respectively. After removing all solvents under vacuum, the residue was dissolved in 50 ml toluene and filtered over Celite. Evaporation of the toluene yielded nearly pure solid

products which can be re-crystallised from toluene (**4b**, **4c** and **7**) or Et_2O (**4a**) (yields >90%).

***BABAR*-Phos 5a, 5b and 5d**. A solution of **4a**, **4b** or **4c** (29 mmol) in 100 ml THF was stirred in presence of 1 g (41 mmol) Mg turnings at room temperature. After 5 h, 5 ml of dry dioxane were added to precipitate $MgCl_2$. The solvents were evaporated, the residue was dissolved in 100 ml toluene and filtered over Celite. The toluene phase was concentrated to 10% of its volume and hexane was added to precipitate spectroscopically pure **5a** or **5b**. Compound **5c** could not be isolated prior to polymerisation in concentrated solutions.

8. A solution of 1 g of **7** (2.7 mmol) in 5 ml CH_2Cl_2 was added to a vigorously stirred suspension of 0.4 g $AlCl_3$ (3 mmol) in 20 ml CH_2Cl_2 at −78°C. The solution was filtered and the solvent removed in vacuo to give 1.3 g (2.6 mmol) **7** (98%) as a white micro-crystalline powder. Crystals suitable for an X-ray crystal structure determination were obtained by re-crystallisation from a saturated CH_2Cl_2 solution.

11a and 11b. Platinum complex **11a** was obtained in 70% yield (97 mg) by mixing 53 mg (0.11 mmol) $[Pt(nbn)_3]$ (**9**), 50 mg (0.27 mmol) dvtms (**10**) and 60 mg (0.21 mmol) **5a** in 2 ml toluene. Crystals were grown from concentrated hexane solutions. Complex **11b** was prepared in the same manner but its isolation failed because of decomposition in the absence of excess dvtms. Although decomposition during work-up took place, **11b** could be fully characterised by NMR-spectroscopy in the presence of excess dvtms. Some crystals of **11b** were grown out of hexane and could be isolated beside oily products resulting from decomposition.

13. To a solution of 100 mg (0.21 mmol) **9** and 21 mg (0.21 mmol) maleic anhydride **12** in 2 ml toluene, 96 mg (0.21 mmol) **5b** dissolved in 2 ml toluene were added. After 30 min the solvent and free nbn were removed in vacuo. The resulting beige powder was washed 2 times with 0.5 ml benzene to give 130 mg (1.6 mmol, 75%) **13** as white crystalline powder after drying in vacuo.

21. To a solution of 100 mg (0.21 mmol) **9** and 20 mg (0.11 mmol) dvtms in 2 ml hexane was added dropwise a solution of **5b** in 2 ml benzene. After a few seconds **21** starts to precipitate as yellow micro crystalline powder which was filtered off and washed with 2 ml hexane. After drying in vacuo 160 mg (0.08 mmol, 78%) of pure **21** were obtained. Layering a concentrated THF solution with hexane yielded crystals suitable for an X-ray analysis.

References

1. For recent calculations see: (a) Bode, B. M.; Day, P. N.; Gordon, M. S. *J. Am. Chem. Soc.* **1998**, *120*, 1552 and references therein. (b) Sakaki, S.; Ogawa, M.; Musashi, Y.; Arai, T. *J. Am. Chem. Soc.* **1994**, *116*, 7258. (c) Sakaki, S.; Ikeki, M. *J. Am. Chem. Soc.* **1993**, *115*, 2373. (d) An overview about some experimental aspects is given by: Lewis, L. N.; Sy, K. G.; Bryant, Jr., G. L.; Donahue, P. E. *Organometallics* **1991**, *10*, 3750 and references therein.

2. (a) Albright, T. A.; Burdett, J. K.; Whangbo, M.-H. *Orbital Interactions in Chemistry;* Wiley: New York, 1985; p 140. (b) Dunne, B. J.; Morris, R. B.; Orpen, A. G. *J. Chem. Soc., Dalton Trans.* **1991**, *653* and references therein.

3. Recent reviews: (a) Dillon, K. B.; Mathey, F.; Nixon, J. F. *Phosphorus: The Carbon Copy;* Wiley: New York, 1998; p 182. (b) Mathey, F.; Regitz, M. *Comprehensive Heterocyclic Chemistry II;* Padwa, A., Ed.; Elsevier: Amsterdam, 1996; p 277. (c) Mathey, F. *Chem. Rev.* **1990**, *90*, 997.

4. Only selected recent publications are given here which point out the names of research groups involved the synthesis and chemistry of phosphiranes: (a) Mézailles, N.; Fanwick, P. E.; Kubiak, C. P. *Organometallics* **1997**, *16*, 1526. (b) Li, X.; Robinson, K. D.; Gaspar, P. P. *J. Org. Chem.* **1996**, *61*, 7702. (c) Hockless, D. R.; Kang, Y.; McDonald, M. A.; Pabel, M.; Willis, A. C.; Wild, S. B. *Organometallics* **1996**, *15*, 1301. (d) Marinetti, A.; Ricard, L.; Mathey, F. *Synthesis* **1992**, 157. (e) Marinetti, A.; Mathey, F. *Tetrahedron Lett.* **1987**, *28*, 5021. (f) Tsuji, K.; Sasaki, S.; Yoshifuji, M. *Heteroat. Chem.* **1998**, *7*, 607. (g) Review: Mathey, F. *Angew. Chem.* **1987**, *99*, 285; *Angew. Chem., Int. Ed. Engl.* **1987**, *26*, 275. (h) Krill, S.; Wang, B.; Hung, J.-T.; Horan, C. J.; Gray, G. M.; Lammertsma, K. *J. Am. Chem. Soc.* **1997**, *119*, 8432. (i) Becker, P.; Brombach, H.; David, O.; Leuer, M.; Metternich, H.-J.; Niecke, E. *Chem. Ber.* **1992**, *125*, 771. (j) Kolodiazhnyi, O. I.; Gishkun, V. E. *Heteroat. Chem.* **1998**, *9*, 659. (k) Yoshifuji, M.; Toyota, K.; Yoshimura, H.; Hirotsu, K.; Okamoto, A. *J. Chem. Soc., Chem. Commun.* **1991**, 124. (l) Manz, B.; Maas, G. *J. Chem. Soc., Chem. Commun.* **1995**, 25. (m) Lentz, D.; Marschall, R. *Z. Anorg. Allg. Chem.* **1992**, *617*, 53. (n) Yoshifuji, M.; Yoshimura, H.; Toyota, K. *Chem. Lett.* **1990**, 827. (o) Schnurr, W.; Regitz, M. *Tetrahedron Lett.* **1989**, *30*, 3951. (p) Märkl, G.; Hohenweider, K.; Ziegler, M. L.; Nuber, B. *Tetrahedron Lett.* **1990**, *31*, 4849. (q) Märkl, G.; Hölzl, W. *Tetrahedron Lett.* **1989**, *30*, 4501. (r) Zablocka, M.; Miquel, Y.; Igau, A.; Majoral, J. P.; Skowronska, A. *J. Chem. Soc., Chem. Commun.* **1998**, 1177.

5. [2+1] cycloreversions: (a) Gaspar, P. P.; Li, X.; Silverman, J.; Haile, T.; Pae, D. H.; Xiao, M. *Prog. Organosilicon Chem. (Jubilee Int. Symp. Organosilicon Chem.)*, 10th ed.; Mariniec, B., Chojnowski, J., Eds.; 1995; p 247. (b) Li, X.; Weissman, S. I.; Lin, T.-S.; Gaspar, P. P. *J. Am. Chem. Soc.* **1994**, *116*, 7899 and references therein. (c) Retro-electrocyclisation: Chaquin, P.; Gherbi, A. *J. Org. Chem.* **1995**, *60*, 3723. (d) Ring–chain rearrangements: Nguyen, M. T.; Landuyt, L.; Vanquickenborne, L. G. *J. Chem. Soc., Faraday Trans.* **1994**, *90*, 1771. (e) Recent reports on thermal rearrangements of phosphirane complexes: Wang, B.; Lake, C. H.; Lammertsma, K. *J. Am. Chem. Soc.* **1996**, *118*, 1690. (f) Huy, N. H. T.; Mathey, F. *Synlett.* **1995**, 353. (g) Flash pyrolysis of phosphiranes: Haber, LeFloch, P.; Mathey, F. *Phosphorus, Sulfur and Silicon* **1993**, *75*, 225. (h) Kobayashi, S.; Kadokawa, J.-I. *Marcomol. Rapid Commun.* **1994**, *15*, 567; Surface phosphinidenes [RP(Mg] have been proposed: Bock, H.; Bankmann, M. *J. Chem. Soc., Chem. Commun.* **1989**, 1130.

6. Marinetti, A.; Mathey, F.; Ricard, L. *Organometallics* **1993,** *12*, 1207.

7. (a) **C**: Binger, P.; Leisinger, S.; Regitz, M.; Bergsträsser, U.; Bruckmann, J.; Krüger, C. *J. Organomet. Chem.* **1997**, *529*, 215 and references therein. (b) **D**: Hu, D.; Schäufele, H.; Pritzkow, H.; Zenneck, U. *Angew. Chem.* **1989**, *101*, 929; *Angew. Chem., Int. Ed. Engl.* **1989**, *28*, 900. (c) **E**: Avarvari, N.; Ricard, L.; Mathey, F.; Le Floch, P.; Löber, O.; Regitz, M. *Eur. J. Org. Chem.* **1998**, 2039. (d) F: Heydt, H.; Bergsträsser, U.; Fässler, R.; Fuchs, E.; Kamel, N.;

Mackewitz, T.; Michels, G.; Rösch, W.; Regitz, M.; Mazerolles, P.; Laurent, C.; Faucher, A. *Bull. Soc. Chim. Fr.* **1995**, *132*, 652. (e) Also, P4 (**G**) is a quite stable molecule.

8. Liedtke, J.; Loss, S.; Alcaraz, G.; Gramlich, V.; Grützmacher, H. *Angew. Chem.* **1999**, *111*, 1724; *Angew. Chem. Int. Ed. Engl.* **1999**, *38*, 1623.

9. (a) Hockless, D. C. R.; McDonald, M. A.; Pabel, M.; Wild, S. B. *J. Organomet. Chem.* **1997**, *529*, 189. (b) For π-exchange reactions of phosphiranium salts see: Sølling, T. I.; McDonald, M. A.; Wild, S. B.; Radom, L. *J. Am. Chem. Soc.* **1998**, *120*, 7063.

10. Nguyen, M. T.; Van Praet, E.; Vanquickenborne, L. G. *Inorg. Chem.* **1994**, *33*, 1153.

11. Pregosin, P. S. *Annual Reports on NMR Spectroscopy* **1986**, *17*, 285.

12. Al Juaid, S. S.; Carmichael, D.; Hitchcock, P. B.; Marinetti, A.; Mathey, F.; Nixon, J. A. *J. Chem. Soc., Dalton Trans.* **1991**, 905.

13. (a) Carmichael, D.; Hitchcock, P. B.; Nixon, J. F.; Mathey, F.; Ricard, L. *J. Chem. Soc., Dalton Trans.* **1993**, 1811 and references therein. (b) Ajulu, F. A.; Hitchcock, P. B.; Mathey, F.; Michelin, R. A.; Nixon, J. A.; Pombeiro, A. J. L. *J. Chem. Soc., Chem. Commun.* **1993**, 142.

14. **4a**: Triclinic, space group P1(Bar); a=11.1247(3), b=11.9546(3), c=14.8553(4) Å, α=105.010(1), β=101.051(1), y=106.338(1)°; V=1755.00(8) Å^3; Z=2, MoK$_\alpha$-radiation, $2\Theta_{max}$=49.4°. 11185 reflections, 5935 independent ($R_{int.}$=0.0328); R_1=4.48%, wR_2=10.80% (based on F^2) for 397 parameters and 4244 reflections with $I>2\sigma(I)$. **8**: Orthorhombic, space group *Pnma*; a=18.4162(6), b=11.7414(4), c=11.9241(4) Å; V=2578.4(2) Å^3; Z=4, MoK$_\alpha$-radiation, $2\Theta_{max}$=46.5°. 13763 reflections, 1959 independent ($R_{int.}$=0.0555); R_1=4.33%, wR$_2$=9.91% (based on F^2) for 166 parameters and 1421 reflections with $I>2\sigma(I)$. **11b**: Monoclinic, space group $P2_1/c$; a=12.4110(3), b=13.3071(3), c=19.9116(5) Å, β=94.848(1)°; V=3276.7(1) Å^3; Z=4, MoK$_\alpha$-radiation, $2\Theta_{max}$=56.6°. 26 804 reflections, 8117 independent ($R_{int.}$=0.0613); R_1=3.21%, wR_2=7.10% (based on F^2) for 388 parameters and 5992 reflections with $I>2\sigma(I)$. **13**: Triclinic, space group $P1$(bar); a=11.1323(5), b=11.4105(4), c=13.3558(4) Å, α=68.374(1), β=77.122(2), y=84.763(1)°; V=1537.4(1) Å^3; Z=2, MoK$_\alpha$-radiation, $2\Theta_{max}$=56.6°. 6780 reflections, 5333 independent ($R_{int.}$=0.0459); R_1=5.99%, wR_2=14.18% (based on F^2) for 386 parameters and 3598 reflections with $I>2\sigma(I)$. **21**: Monoclinic, space group $P2_1$/n; a=12.7945(5), b=25.6583(10), c=24.2287(9) Å, β=95.005(1)°; V=7923.6(5) Å^3; Z=4, MoK$_\alpha$-radiation, $2\Theta_{max}$=52.7°. 48355 reflections, 16125 independent ($R_{int.}$=0.0890); R_1=5.42%, wR_2=10.17% (based on F^2) for 993 parameters and 9944 reflections with $I>2\sigma(I)$. All structures were solved by direct methods and refined against full matrix (versus F^2) with SHELXTL (Version 5.0). Non-hydrogen atoms were refined isotropically, hydrogen atoms were refined on calculated positions using the riding model. The isopropyl group in structure **8** as well as one CF_3-group in **11b** and **21** were disordered over 2 or 3 positions, respectively. In structure **21** five partially occupied atoms equivalent to carbon were refined to describe one disordered THF molecule. Crystallographic data (excluding structure factors) for the structures reported in this paper have been deposited with the Cambridge Data Centre as supplementary publication nos. CCDC-119359 (**4a**); 106558 (**8**); 119356 (**11b**); 119357 (**13**); 119358 (**21**). Copies of the data can be obtained free of charge on application to CCDC, 12 Union Road, Cambridge, CB21EZ, UK (fax: +44-1223-336-033; e-mail: deposit@ccdc.cam.ac.uk).

15. (a) Chandra, G.; Lo, P. Y.; Hitchcock, P. B.; Lappert, M. F. *Organometallics* **1987**, *6*, 191. (b) Hitchcock, P. B.; Lappert, M. F.; Warhurst, N. J. W. *Angew. Chem.* **1991**, *103*, 439; *Angew. Chem., Int. Ed. Engl.* **1991**, *30*, 438.

16. A reaction catalysed by such a catalyst may be called Park&Ride catalysis and finds prominent precedence in biological systems.

17. Kessler, H. In *Methoden der Organischen Chemie, (Houben-Weyl);* Müller, E., Ed.; Thieme: Stuttgart, 1972; Vol. 5/1d, p 301.